Phase-sensitive γ-encoded recoupling of heteronuclear dipolar interactions and ^{1}H chemical shift anisotropy

Frédéric A. Perras,[1]* Alexander L. Paterson[1], Takeshi Kobayashi[1]

[1]US DOE, Ames Laboratory, Ames, IA 50011, USA

Abstract

γ-encoded recoupling sequences are known to produce strong amplitude modulations that lead to sharp doublets when Fourier transformed. These doublets depend very little on the recoupled tensor asymmetry and thus and enable for the straightforward determination of dynamic order parameters. It can, however, be difficult to measure small anisotropies, or small order parameters, using such sequences; the resonances from the doublet may overlap with each other, or with the zero-frequency glitch. This limitation has prevented the widespread use of ^{1}H chemical shift anisotropy (CSA) for the measurement of dynamics, particularly for CH protons which typically have CSAs of only a few ppm when immobile. Here, we introduce a simple modification to the traditional ^{1}H CSA and proton-detected local field pulse sequences that enables the acquisition of a hypercomplex dataset and the removal of the uncorrelated magnetization that results in the zero-frequency glitch. These new sequences then yield a frequency shift in the indirect dimension, rather than a splitting, which is easily identifiable even in cases of weak interactions.

Graphical Abstract

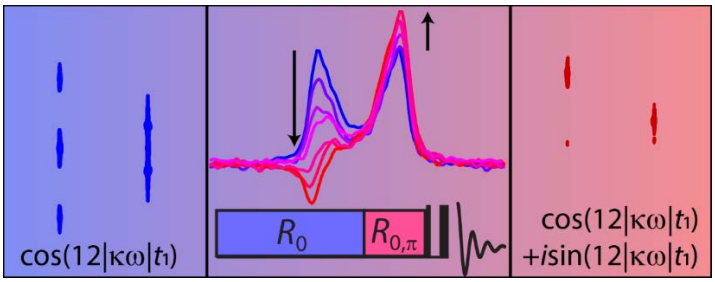

1. Introduction

Dynamics play a large role in many fields including biochemistry,[1,2] battery chemistry,[3,4] and catalysis[5,6] to name a few. Characterizing these dynamics, however, is often a challenge: most tools are either insensitive to motions, particularly conformational dynamics; or are limited to the study of motions in a very limited timescale. Solid-state nuclear magnetic resonance (SSNMR) spectroscopy is less burdened by most of these limitations and is often the tool of choice for the study of dynamics, particularly in the case of biomacromolecules.[7] In particular, the measurement of averaged interaction tensors enables for the orientational space of a given site to be evaluated so long as the motions occur at a faster rate than the breadth of the anisotropic interaction (typically on the order of kHz). Slower motions can, of course, also be probed through two-dimensional exchange experiments.

Regardless of the motional mode, the dynamic averaging of an interaction tensor always leads to the weakening of its anisotropic part, down to zero in the case of isotropic motions.[8] For this reason, it is generally easiest to probe dynamics using larger anisotropic interactions such as the ^{2}H quadrupolar coupling tensor, which is regarded as the gold standard for the study of dynamics in solids.[9] The progressive weakening of anisotropic interactions as motions increase in amplitude is often summarized using the so-called order parameter $\langle S \rangle$ which is simply the fraction of the anisotropic part of the static tensor remaining in the presence of motions.[10]

A second factor that makes ^{2}H SSNMR a particularly good probe of dynamics is the predictability of its electric field gradient tensor.[11] It is generally true that the largest tensor component is oriented along the ^{2}H-X bond and the magnitude of the interaction is fairly consistent for similar moieties. This is not the case, for instance, with ^{13}C chemical shift tensors[12] which often need to rely on quantum chemical calculations for interpretation.[13] The ubiquity of hydrogen in most systems also means that multiple ^{2}H order parameters can be measured in a given system to enable the determination of more complex motional modes.

Two parameters share these latter advantages of ^{2}H quadrupolar coupling, namely, the ^{1}H-X dipolar coupling interaction and the ^{1}H chemical shift anisotropy (CSA). ^{1}H CSA, in particular, has hardly been explored in this context.[14] The limiting factor that has slowed the adoption of ^{1}H NMR for the study of dynamics, more so in the case of CSA, is that any recoupling method must not only recouple the chosen interaction under magic angle spinning (MAS) but also prevent the interference of the stronger ^{1}H homonuclear dipolar interactions.

Aside from a few examples using rotary resonance[15] and CSA amplification,[16] measurements of ^{1}H CSA have generally been performed using γ-encoded, *R*-type, symmetry-based recoupling.[14,17 -25] One of the main strengths of the γ-encoded sequences is that they produce very pronounced oscillations that, when Fourier transformed, reveal a doublet that directly reflects $\langle S \rangle$, since the splitting is largely insensitive to the asymmetry of the tensor.[19,26] In cases when the interaction is weak, such as in the presence of large amplitude motions, the two peaks in the doublet can overlap with each other and the zero-frequency glitch (which originates from uncorrelated magnetization) thus preventing the measurement of the interaction entirely. Weaker

C-H ^{1}H CSAs have only been measured using such sequences and mostly at very high magnetic fields.[17,20-22]

In this work we build on Veglia's phase-sensitive variants of the static separated local field experiments,[27,28] such as SE-PISEMA, and develop phase-sensitive variants of the ^{1}H CSA recoupling experiment as well as the proton-detected local field (R-PDLF)[29] dipolar-shift correlation experiment. These methods rely on the acquisition of two, phase-shifted, datasets that can be recombined to generate a hypercomplex signal and processed via the States method.[30] The result is the elimination of one of the members of the doublet. This procedure ensures measurable frequency shifts, even in cases when the recoupled doublet is not resolved, facilitating the measurement of weak interactions.

2. Theory

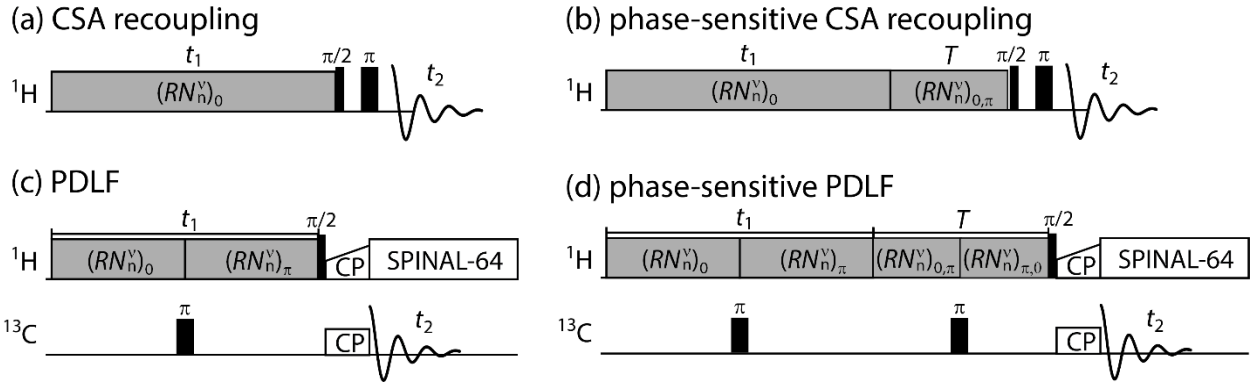

Figure 1. Pulse sequence diagrams for the conventional (a) and phase-sensitive (b) symmetry-based ^{1}H CSA recoupling experiments as well as the conventional (c) and phase-sensitive (d) R-PDLF experiments.

The pulse sequences discussed in this paper are shown in Figure 1. If we take the simplest sequence, shown in Figure 1a, we see that the recoupling is applied to longitudinal ^{1}H magnetization. This recoupling leads to the modulation of this magnetization as follows:[31,32]

$$I_z \rightarrow I_z \cos(12|\kappa\omega_i|t_1) - 2I_y \sin(12|\kappa\omega_i|t_1) \quad (1)$$

where ω_i depends of the reduced anisotropy of the chemical shift tensor ($\omega_{aniso} = \omega_0\delta_{ani} = \omega_0(\delta_{zz} - \delta_{iso})$, where: $|\delta_{zz} - \delta_{iso}| \geq |\delta_{xx} - \delta_{iso}| \geq |\delta_{xx} - \delta_{iso}|$ and ω_0 is the Larmor frequency in angular units) in the case of CSA recoupling and the dipolar coupling constant ($\omega_{ij} = -\mu_0\gamma_1\gamma_2\hbar(4\pi)^{-1}r_{ij}^{-3}$) in the case of R-PDLF, as well as the orientation of the tensor in the magnetic field. κ corresponds to the scaling factor of the recoupling sequence used. Note that in the case of dipolar recoupling the second term takes the form of I_yS_z.

Following the recoupling, the longitudinal ^{1}H magnetization (the first term in equation 1) is excited by a $\pi/2$ pulse, leading to a two-dimensional dataset of the form:

$$\cos(12|\kappa\omega_i|t_1)\left[I_x\cos(\omega_{iso}t_2) + I_y\sin(\omega_{iso}t_2)\right] \quad (2)$$

where ω_{iso} is the isotropic chemical shift that evolves freely during t_2. Experimentally an echo is also used to reduce probe background signals. Since this acquisition procedure discards the sine-modulated term in equation 1, the dataset is not phase-sensitive and a symmetric doublet is obtained in the indirect dimension of the two-dimensional spectrum.

The R-PDLF experiment, depicted in Figure 1c, functions in the same way; however, the phase of the recoupling is reversed in a second recoupling period to refocus the ^{1}H CSA. An inversion pulse applied to the heteronuclide prevents the same from occurring in the case of the dipolar coupling, yielding a pure dipolar cosine-modulated signal (equation 2).

Returning to equation 1, if we then introduce a second recoupling period of duration T (see Figures 1b and 1d) we obtain

$$I_z[\cos(12|\kappa\omega_i|t_1)\cos(12|\kappa\omega_i|T) + \sin(12|\kappa\omega_i|t_1)\sin(12|\kappa\omega_i|T)] - 2I_y[\sin(12|\kappa\omega_i|t_1)\cos(12|\kappa\omega_i|T) - \cos(12|\kappa\omega_i|t_1)\sin(12|\kappa\omega_i|T)] \quad (3)$$

when the phase of the second recoupling period matches that from the first, and

$$I_z[\cos(12|\kappa\omega_i|t_1)\cos(12|\kappa\omega_i|T) - \sin(12|\kappa\omega_i|t_1)\sin(12|\kappa\omega_i|T)] - 2I_y[\sin(12|\kappa\omega_i|t_1)\cos(12|\kappa\omega_i|T) + \cos(12|\kappa\omega_i|t_1)\sin(12|\kappa\omega_i|T)] \quad (4)$$

when the phase is reversed. Again, only the first term is detected following the recoupling and the two dimensional datasets take the form

$$[\cos(12|\kappa\omega_i|t_1)\cos(12|\kappa\omega_i|T) + \sin(12|\kappa\omega_i|t_1)\sin(12|\kappa\omega_i|T)]\left[I_x\cos(\omega_{iso}t_2) + I_y\sin(\omega_{iso}t_2)\right] \quad (5)$$

$$[\cos(12|\kappa\omega_i|t_1)\cos(12|\kappa\omega_i|T) - \sin(12|\kappa\omega_i|t_1)\sin(12|\kappa\omega_i|T)]\left[I_x\cos(\omega_{iso}t_2) + I_y\sin(\omega_{iso}t_2)\right] \quad (6)$$

The sum of these two time domain signals produces a pure cosine-modulated signal in t_1, similarly to equation 2,

$$2\cos(12|\kappa\omega_i|t_1)\cos(12|\kappa\omega_i|T)\left[I_x\cos(\omega_{iso}t_2) + I_y\sin(\omega_{iso}t_2)\right] \quad (7)$$

and their difference produces a pure sine-modulated signal.

$$2\sin(12|\kappa\omega_i|t_1)\sin(12|\kappa\omega_i|T)\left[I_x\cos(\omega_{iso}t_2) + I_y\sin(\omega_{iso}t_2)\right]. \quad (8)$$

The amplitude of the cosine signal is decreased by $\cos(12|\kappa\omega_i|T)$ while that of the previously unobservable sine signal is increased to $\sin(12|\kappa\omega_i|T)$. Setting T to 0 corresponds to the usual, cosine-modulated experiments, which yields an in-phase doublet when Fourier transformed, and setting T such that $12|\kappa\omega_i|T = \pi/2$ will produce a pure sine-modulated signal and an anti-phase doublet in the frequency domain. If T is set such that $12|\kappa\omega_i|T = \pi/4$ all intensity is condensed into a single peak with an amplitude increased by a factor of $\sqrt{2}$. In practice, however, while the amplitude of the signal is increased, the signal-to-noise ratio is not enhanced since in the case of the pure cosine-modulated experiment the sine signals can be zeroed to reduce the noise level by the same factor. We lastly note that the sine signal is only a reconstruction, using the modulation

of I_z, and does not correspond to the sine modulation the I_y (or I_yS_z in the dipolar case). As such the sign of the precession has no meaning and these sequences cannot be used to distinguish the skew of the chemical shift tensor, for instance.

The phase-sensitive approaches do, however, provide unique advantages in resolution. Specifically, while the center of mass of the doublet is always centered at zero in the conventional 2D spectrum, it is shifted in the phase-sensitive spectrum, even in cases of spectral overlap, thus providing a mechanism for the measurement of weak interactions. In addition, while the phase of the doublet can be altered by the sequences depicted in Figures 1b and 1d, the uncorrelated magnetization is always manifested as a positive peak of zero-frequency. As such, if a sine-modulated experiment (Figure 1b and 1d with $12|\kappa\omega_i|T = \pi/2$) is subtracted from the usual pure cosine-modulated experiment (Figures 1a and 1c), the uncorrelated signal can be removed, in addition to one of the members of the doublet.

3. Experimental

All experiments were performed on a Varian VNMRS 600 MHz solid-state NMR spectrometer. ^{1}H CSA recoupling measurements on a citric acid sample were performed using a JEOL 0.75 mm ultra-fast MAS probe. The MAS rate was set to 75 kHz and the recoupling used the $R20^8_9(270_090_{180})$ sequence.[22] A radiofrequency power of 166.67 kHz was used for all pulses and the echo duration lasted a single rotor period. Conventional CSA recoupling spectra were acquired using 16 scans per increment and 32 t_1 increments of 120 μs. Phase-sensitive spectra were instead acquired using 8 scans per increment and a total of 32 t_1 complex points (i.e. 64 points in total) such that both experiments acquired a total of 512 scans. The recoupling duration T was varied from 0 to 144 μs; the exact value used for a given spectrum is given in the results and discussion section. The recycle delay was set to 2 minutes. The t_1 decay signal was baseline corrected to minimize the intensity of the zero-frequency glitch. We note that Pandey et al. accomplished a similar result by instead subtracting the average intensity of the last few data points from the rest of the t_1 signal.[22] To determine the δ_{ani} values from a given spectrum, a series of SIMPSON[33] calculations were performed to determine the linear relationship between the observed splitting and the anisotropy of the tensor. For the MAS rate and magnetic field used in our experiments, the relationship was: $\delta_{\mathrm{ani}} = \Delta\nu_{\mathrm{CSA}}(0.0066\ \mathrm{ppm/Hz})$ where $\Delta\nu_{CSA}$ corresponds to the splitting.

R-PDLF experiments were performed using a Varian 3.2 mm MAS probe and a spinning rate of 11.111 kHz. The $R18^5_2(90_0\text{-}\tau\text{-}90_0)$ sequence[34,35] with a 50% window duration τ was used, requiring 100 kHz ^{1}H pulses. The windowed R element both increases the scaling factor of the recoupling sequence[36] as well as reduces its sensitivity to radiofrequency imperfections and maladjustments.[37,38] Polarization transfer to ^{13}C was effected via cross-polarization. A tangent pulse was applied at the ^{1}H frequency and the contact time lasted 150 μs. Conventional R-PDLF experiments were acquired using 64 scans for alanine and 256 scans for N-formyl-Met-Leu-Phe (MLF) and a total of 64 t_1 increments. The number of scans per increment was again halved for the case of the phase-sensitive experiments, and 64 complex t_1 points (i.e. 128 points in total) were acquired. Recycle delays of 4 and 5 seconds were used for alanine and MLF, respectively. The t_1 decay signal was baseline corrected to minimize the intensity of the zero-frequency glitch.

The produced two-dimensional free induction decays (FIDs) were converted to the form required for hypercomplex processing[30] (see Theory section) using the C programs provided as supplementary information. The first (ser-symmetrize.c) inserts zeroes in between the individual t_2 FIDs to act as a zeroed sine signal. The second (ser-convert.c) takes the sum and difference between the successive FIDs to generate the pure cosine and sine signals.

4. Results and Discussion

4.1. ^{1}H CSA Recoupling

To test the ideas outlined in the Theory section we have used citric acid, whose ^{1}H CSA has been investigated at slow and ultrafast MAS rates.[17,19,22] Citric acid features both hydroxyl protons, that have relatively large CSAs, as well as aliphatic (CH_2) protons with weaker CSAs. It is worth mentioning that prior studies were performed at higher magnetic field strengths corresponding to ^{1}H Larmor frequencies of 700, 850, and 900 MHz, where the CSA is 17 to 50% stronger in frequency units than it is in the case of our spectrometer (600 MHz).

Recoupled CSA spectra from the highest chemical shift (13.9 ppm) acid site are shown in Figure 2 as a function of the duration of the recoupling period *T*. *T* was varied from 0 to 144 μs in steps of 24 μs. As can be seen, increasing the duration of *T* leads to the suppression, and eventual inversion, of one of the two signals in the doublet, while some of the intensity is folded into the second, positive, peak.

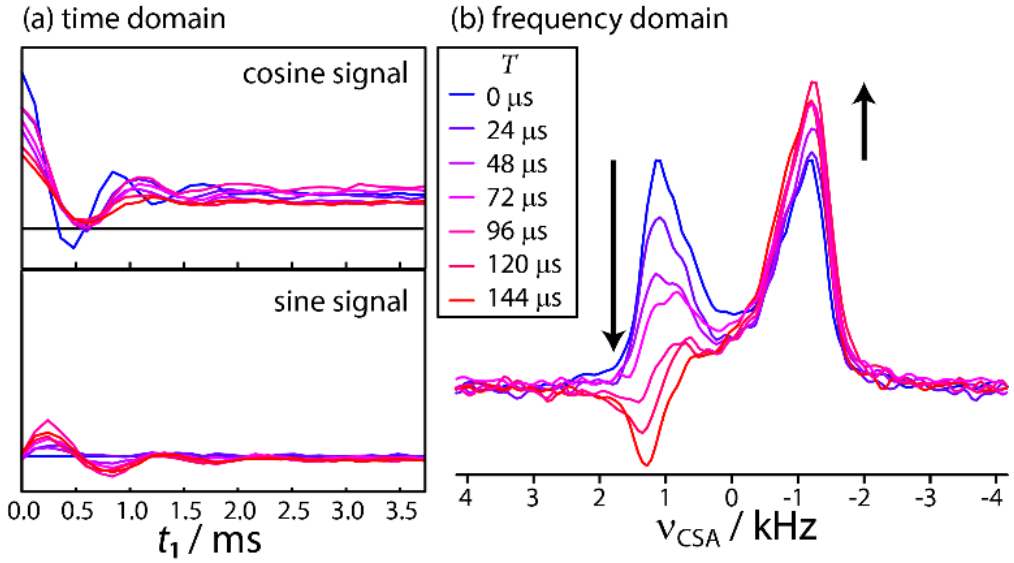

Figure 2. Impact of changing the constant recoupling time duration *T* from 0 (blue) to 144 μs (red) in the case of the highest-frequency ^{1}H resonance of citric acid. The cosine- and sine-modulated time domain signals are shown in (a) while the corresponding frequency-domain spectra are shown in (b).

The full two-dimensional spectra acquired with *T* set to 0 μs (conventional) and 120 μs (phase-sensitive) are shown in Figure 3a and b, respectively. As expected, the splittings introduced from the CSA are easily observed for the four hydroxyl signals. The case is different, however, for

the CH_2 protons whose CSA-recoupled spectra are broad and featureless when the conventional CSA recoupling experiment is used. This is not the case with the phase-sensitive experiment, which shows a clear shift of the center of gravity in the indirectly-detected CSA spectrum that can only arise from the recoupled CSA. The values of δ_{ani} extracted from the peak maxima in Figure 3c are given in Table 1 and are in good agreement with those from prior literature.[17,19,22]

Table 1. ^{1}H δ_{ani} values determined for citric acid.

site	δ_{iso} / ppm	δ_{ani} / ppm				
		conventional	phase-sensitive	ref. [17]	ref. [19]	ref. [22]
-COOH	13.9	16.1 ± 0.4	16.1 ± 0.4	17.9 ± 0.7	16.9 ± 0.4	16.6
-COOH	10.7	12.5 ± 0.3	12.6 ± 0.3	12.5 ± 0.4	12.5 ± 0.3	12.5
-COOH	10.0	12.5 ± 0.3	12.6 ± 0.3	12.8 ± 0.5	12.5 ± 0.3	12.5
-OH	5.5	13.3 ± 0.3	13.6 ± 0.3	14.0 ± 0.5	13.6 ± 0.6	13.4
$-CH_2-$	3.1	--	7.2 ± 0.8	5.5 ± 0.5	--	6.8
$-CH_2-$	2.4	--	6.7 ± 0.8	4.5 ± 0.5	--	6.5

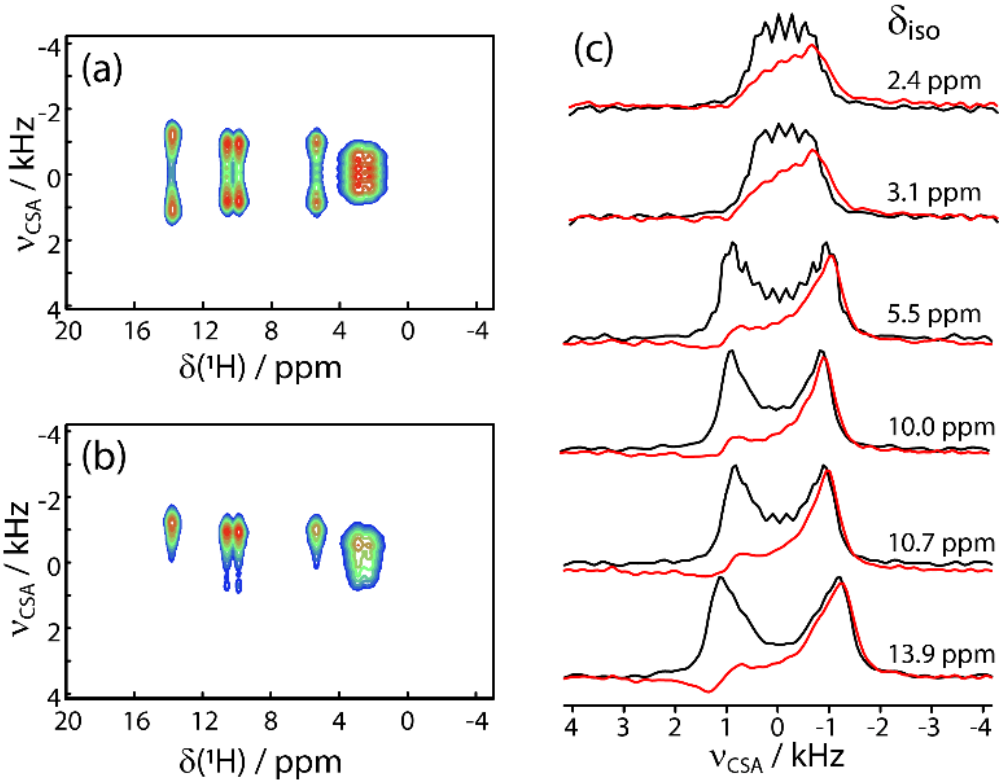

Figure 3. Two-dimensional ^{1}H CSA recoupling spectrum acquired on citric acid with an MAS rate of 75 kHz using the $R20^8_9(270_090_{180})$ sequence. The result of the conventional experiment is depicted in (a) while that from the phase-sensitive sequence is given in (b). The phase-sensitive sequence used a recoupling period, T, of 120 μs. Slices taken along the indirect dimension of the 2D spectrum for all six resonances are shown in (c) with the conventional spectrum shown in black and the phase-sensitive one shown in red. The spectra are scaled to the same noise level and were both acquired with the same total acquisition time.

For all six sites, the sensitivity per time was comparable in both experiments, indicating that the additional 120 μs of recoupling did not lead to significant, non-refocussable, signal decay.

4.2. $^{1}H\{^{13}C\}$ R-PDLF

The same approach can be used to recouple ^{1}H-^{13}C dipolar interactions in a phase-sensitive manner; however, in this case it is also important to refocus the ^{1}H CSA to limit its interference. This is accomplished by shifting the phase of the recoupling block by π, which serves to refocus both the CSA and the heteronuclear dipolar interactions.[29,32] The aforementioned refocusing of the dipolar interaction can, however, be prevented by the application of a ^{13}C inversion pulse (R-PDLF sequence, Figure 1c).

Here we chose to use the R-PDLF experiment in particular since, unlike approaches that apply the heteronuclear recoupling during a ^{13}C evolution period,[39,40,41,42] in R-PDLF the same doublet is expected regardless of the number of hydrogen atoms bound to the carbon. In other words, CH_3, CH_2, and CH groups all produce the same recoupled spectrum since in all cases each ^{1}H spin only sees a single ^{13}C spin.

To test the phase-sensitive R-PDLF sequence, we used alanine, which features a rigid CH moiety, a rotating methyl group, and a non-protonated carboxyl; the spectra are shown in Figure 4. The first spectrum, in Figure 4a, corresponds to the usual R-PDLF spectrum and displays a doublet for each of the protonated sites. The recoupled splittings are 7.8 and 2.5 kHz wide for the CH and CH_3 sites, with the 1/3 reduced splitting of the methyl resonance being indicative of free methyl rotation.[43] In contrast with the CSA recoupling measurements from the previous section, the baseline correction of the t_1 decay signal was unsuccessful in completely suppressing the zero-frequency glitch, possibly due to its non-Lorentzian shape

The spectrum acquired using the phase-sensitive sequence (Figure 1d) is shown in Figure 4b. There a minimum recoupling period T of 40 μs was used. One of the resonances in the doublets is efficiently suppressed while the other is reduced by approximately 20%. The zero-frequency glitch is also still prominent, with roughly the same relative amplitude.

In a third experiment (Figure 4c) we doubled T to 80 μs which led to the inversion of the lower-frequency peak in the doublet. This spectrum can then be subtracted from that acquired with the conventional sequence to cancel both the high-frequency member of the doublet as well as the zero-frequency glitch (blue traces in Figure 4d). The residual, unmodulated, signal from the quaternary carboxyl carbon is also suppressed, yielding a cleaner R-PDLF spectrum with a single resonance for each site.

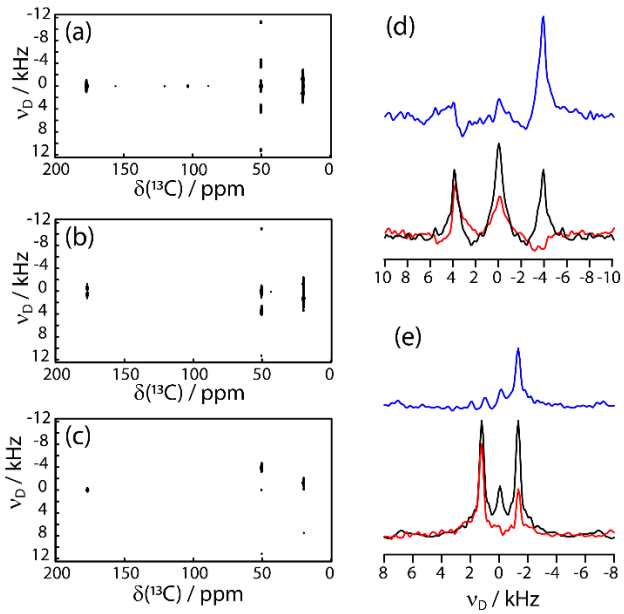

Figure 4. Two-dimensional $^{13}C\{^1H\}$ R-PDLF spectra acquired on alanine with an MAS rate of 11.111 kHz using the $R18^5_2(90_0\text{-}\tau\text{-}90_0)$ sequence. The spectrum obtained with the conventional sequence is shown in (a) while that acquired with the phase-sensitive sequence, and a constant time duration T of 40 μs, is shown in (b). In (c) the spectrum obtained when subtracting a phase-sensitive experiment with a duration T of 80 μs from the conventional spectrum (a) is shown. Shown in (d) and (e) slices are taken along the indirect dimension of the alpha and methyl carbon resonances, respectively. Slices taken from (a), (b), and (c), are shown in black, red, and blue, respectively, and are normalized to the same noise level.

As a final demonstration, we then applied these three approaches to the tripeptide MLF, which features a variety of sites with varying degrees of motional freedom (see Figure 5). [44] A significant fraction of the signal intensity is found in the zero-frequency glitch when the conventional R-PDLF experiment is performed (Figure 5a, Figure S1a), despite the use of FID baseline correction. The phase-sensitive spectrum (Figure S1b) with $T = 40$ μs shows that one half of the spectrum is efficiently suppressed while the other has a signal-to-noise ratio reduced by 5–30 %, depending on the site. The dipolar splittings from the three methyl sites are, however, narrower than that from alanine and are not resolved in either 2D spectrum.

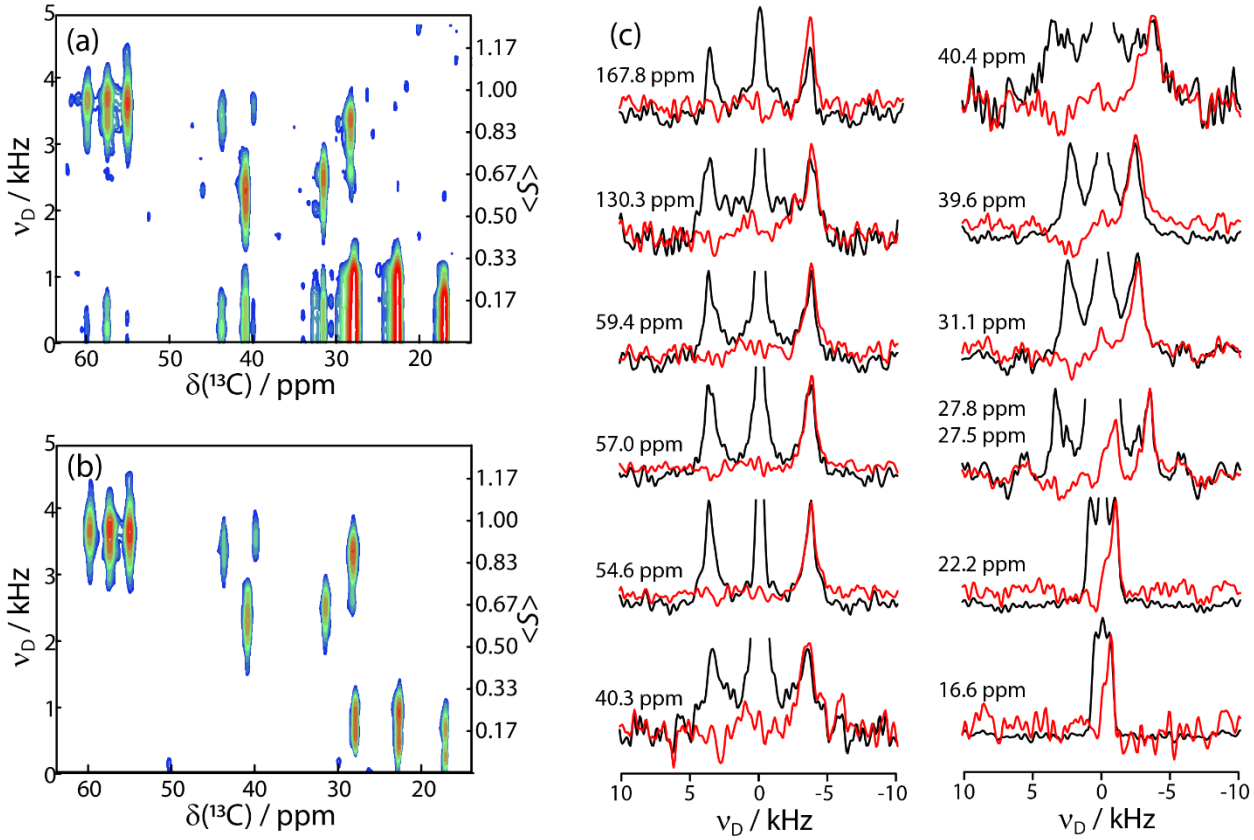

Figure 5. Two-dimensional $^{13}C\{^1H\}$ R-PDLF spectra acquired on MLF with an MAS rate of 11.111 kHz using the $R18^5_2(90_0\text{-}\tau\text{-}90_0)$ sequence. The spectrum obtained with the conventional sequence is shown in (a). In (b) the spectrum obtained when subtracting a phase-sensitive experiment with a duration T of 80 μs from the conventional spectrum (a) is shown. Slices taken along the dipolar dimension for each of the protonated carbons are shown in (c). The black spectra correspond to the conventional R-PDLF spectra (a) while those in red are the phase sensitive results (b).

Using the same approach as used for alanine, we subtracted the anti-phase doublets obtained from the phase-sensitive R-PDLF sequence with T = 80 μs from the in-phase doublet obtained with the conventional R-PDLF sequence to yield the spectrum shown in Figures 5b and S1c. This procedure again largely eliminated the resonances from the quaternary carbon sites as well as the uncorrelated magnetization that obfuscates the dipolar couplings from the methyl sites (see slices in Figure 5c).

As can be seen, with this sequence it is quite straightforward to extract the C-H dipolar order parameters $\langle S \rangle$, including those from the dynamic methyl groups which range from 0.24 to 0.18 (see Table 2 and Figure 5b). These same sites did not have resolved dipolar couplings in a prior study applying the TMREV sequence.[40,44] Comparisons of the dipolar lineshapes measured using this sequence and the more conventional phase-alternating R-symmetry (PARS) experiment,[38,41] where the same recoupling sequence is applied during ^{13}C evolution, are shown in Figures S2 and S3. Generally, the sensitivity of R-PDLF was superior, due to the PARS

experiments being performed in a constant time manner to maximize the resolution. The resolution was nevertheless also much greater in the case of the phase-sensitive R-PDLF since each site leads only to a single resonance, while CH_2 and CH_3 sites have complex multiplet patterns when using PARS. For instance, while two sharp singlets are resolved for the overlapping L_γ and $L_{\delta 1}$ sites when using the phase-sensitive R-PDLF, no discernable splitting is observed when using PARS. It may nevertheless be possible to improve the resolution of PARS by applying the same phase-sensitive approach as we demonstrated for R-PDLF.

Table 2. Dipolar order parameters measured in MLF

site[a]	δ_{iso} / ppm	$\langle S \rangle$[b]
for$_{C'}$	167.8	0.94 ± 0.01
F_ζ	130.3	0.97 ± 0.03
L_α	59.4	0.96 ± 0.02
F_α	57.0	0.97 ± 0.03
M_α	54.6	0.95 ± 0.02
L_β	43.3	0.88 ± 0.05
M_β	40.4	0.61 ± 0.03
F_β	39.6	0.92 ± 0.03
M_γ	31.1	0.66 ± 0.03
L_γ	27.8	0.87 ± 0.04
$L_{\delta 1}$	27.5	0.20 ± 0.05
$L_{\delta 2}$	22.2	0.24 ± 0.07
M_ε	16.6	0.18 ± 0.06

[a]Assignments according to ref [44]. [b]Converted by setting the 7.8 kHz splitting observed in alanine to $\langle S \rangle = 1$.

5. Conclusions

We have shown that by inserting a phase-alternating recoupling period in the conventional ^{1}H CSA recoupling and proton-detected local field (R-PDLF) experiments two recoupled signals that differ in phase can be obtained. These signals can then be recombined to synthesize a hypercomplex dataset and used with States processing to produce phase-sensitive CSA recoupling and R-PDLF spectra. Unlike the conventional recoupling experiments which produce symmetric splittings, the phase-sensitive experiments shift the center of mass of the recoupled signal to enable the measurement of weak anisotropic interactions. Alternatively, one can also combine in-phase and anti-phase recoupled patterns produced by the aforementioned modified sequences and eliminate the zero-frequency glitch along with a member of the doublet. We believe this approach is a meaningful step towards the use of C-H ^{1}H CSA as a probe of dynamic in chemistry and biology where the anisotropies are particularly weak and difficult to resolve by conventional means.

Declaration of Competing Interests

The authors declare that they have no known competing financial interests or personal relationships that could have appeared to influence the work reported in this paper.

Acknowledgements

This work was supported by the U.S. Department of Energy (DOE), Office of Basic Energy Sciences, Division of Chemical Sciences, Geosciences, and Biosciences through a DOE Early Career Project. Ames Laboratory is operated for the DOE by Iowa State University under Contract No. DE-AC02-07CH11358.

References

[1] J. Guo, H.-X. Zhou, Protein allostery and conformational dynamics. Chem. Rev. 116 (2016) 6503-6515.

[2] A. Kohen, Role of dynamics in enzyme catalysis: Substantial versus semantic controversies. Acc. Chem. Res. 48 (2015) 466-473.

[3] C. P. Grey, N. Dupré, NMR Studies of cathode materials for lithium-ion rechargeable batteries, Chem. Rev. 104 (2004) 4493-4512,

[4] W. Schmidt, P. Bottke, M. Sternad, P. Gollob, V. Hennige, M. Wilkening, Small change—great effect: Steep increase of Li ion dynamics in $Li_4Ti_5O_{12}$ at the early stages of chemical Li insertion, Chem. Mater. 27 (2015) 1740-1750.

[5] K. F. Kalz, R. Kraehnert, M. Dvoyashkin, R. Dittmeyer, R. Gläser, U. Krewer, K. Reuter, J.-D. Grunwaldt, Future challenges in heterogeneous catalysis: Understanding catalysts under dynamic reaction conditions, ChemCatChem. 9 (2017) 17-29.

[6] H. Zhai, A. N. Alexandrova, Fluxionality of catalytic clusters: When it matters and how to address it, ACS Catal. 7 (2017) 1905-1911.

[7] P. Schanda, M. Ernst, Studying dynamics by magic-angle spinning solid-state NMR spectroscopy: Principles and applications to biomolecules, Prog. Nucl. Magn. Reson. 96 (2016) 1-46.

[8] R. L. Vold, G. L. Hoatson, Effects of jump dynamics on solid state nuclear magnetic resonance line shapes and spin relaxation times, J. Magn. Reson. 198 (2009) 57-72.

[9] H. W. Spiess, Molecular dynamics of solid polymers as revealed by deuteron NMR, Colloid. Polym. Sci. 261 (1983) 193-209.

[10] G. Lipari, A. Szabo, Model-free approach to the interpretation of nuclear magnetic resonance relaxation in macromolecules. 1. Theory and range of validity. J. Am. Chem. Soc. 104 (1982) 4546-4559.

[11] R. G. Barnes, Deuteron quadrupole coupling tensors in solids. In: J. A. S. Smith, Eds. Advances in Nuclear Quadrupole Resonance. Vol. 1. Heyden, London, (1974) 335–355.

[12] R. A. Burton, N. Tjandra, Residue-specific $^{13}C'$ CSA tensor principal components for ubiquitin: Correlation between tensor components and hydrogen Bonding, J. Am. Chem. Soc. 129 (2007) 1321-1326.

[13] F. Blanc, J.-M. Basset, C. Copéret, A. Sinha, Z. J. Tonzetich, R. R. Schrock, X. Solans-Monfort, E. Clot, O. Eisenstein, A. Lesage, L. Emsley, Dynamics of silica-supported catalysts determined by combining solid-state NMR spectroscopy and DFT calculations, J. Am. Chem. Soc. 130 (2008) 5886-5900.

[14] L. Liang, G. Hou, X. Bao, Measurement of proton chemical shift anisotropy in solid-state NMR spectroscopy, Solid State Nucl. Magn. Reson. 93 (2018) 16-28.

[15] L. Duma, D. Abergel, P. Tekely, G. Bodenhausen, Proton chemical shift anisotropy measurements of hydrogen-bonded functional groups by fast magic-angle spinning solid-state NMR spectroscopy, Chem. Commun. (2008) 2361-2363.
[16] Y. Ge, I. Hung, X. Liu, M. Liu, Z. Gan, C. Li, Measurement of amide proton chemical shift anisotropy in perdeuterated proteins using CSA amplification, J. Magn. Reson. 284 (2017) 33-38.
[17] D. H. Brouwer, J. A. Ripmeester, Symmetry-based recoupling of proton chemical shift anisotropies in ultrahigh-field solid-state NMR, J. Magn. Reson. 185 (2007) 173-178.
[18] G. Hou, S. Paramasivam, S. Yan, T. Polenova, A. J. Vega, Multidimensional magic angle spinning NMR spectroscopy for site-resolved measurement of proton chemical shift anisotropy in biological solids. J. Am. Chem. Soc. 135 (2013) 1358-1368.
[19] H. K. Miah, D. A. Bennett, D. Iuga, J. J. Titman, Measuring proton shift tensors with ultrafast MAS NMR, J. Magn. Reson. 235 (2013) 1-5.
[20] G. Hou, R. Gupta, T. Polenova, A. J. Vega, A Magic-angle-spinning NMR spectroscopy method for the site-specific measurement of proton chemical-shift anisotropy in biological and organic solids, Isr. J. Chem. 54 (2014) 171-183.
[21] R. Zhang, K. H. Mroue, A. Ramamoorthy, Proton chemical shift tensors determined by 3D ultrafast MAS double-quantum NMR spectroscopy, J. Chem. Phys. 143 (2015) 144201.
[22] M. K. Pandey, M. Malon, A. Ramamoorthy, Y. Nishiyama, Composite-180° pulse-based symmetry sequences to recouple proton chemical shift anisotropy tensors under ultrafast MAS solid-state NMR spectroscopy, J. Magn. Reson. 250 (2015) 45-54.
[23] M. K. Pandey, Y. Nishiyama, Determination of NH proton chemical shift anisotropy with ^{14}N–^{1}H heteronuclear decoupling using ultrafast magic angle spinning solid-state NMR, J. Magn. Reson. 261 (2015) 133-140.
[24] M. K. Pandey, Y. Nishiyama, Determination of relative orientation between ^{1}H CSA tensors from a 3D solid-state NMR experiment mediated through ^{1}H/^{1}H RFDR mixing under ultrafast MAS, Solid State Nucl. Magn. Reson. 70 (2015) 15-20.
[25] H. K. Miah, R. Cresswell, D. Iuga, J. J. Titman, ^{1}H CSA parameters by ultrafast MAS NMR: Measurement and applications to structure refinement, Solid State Nucl. Magn. Reson. 87 (2017) 67-72.
[26] N. C. Nielsen, H. Bildsøe, H. J. Jakobsen, Double-quantum homonuclear rotary resonance: Efficient dipolar recovery in magic-angle spinning nuclear magnetic resonance, J. Chem. Phys. 101 (1994) 1805-1812.
[27] T. Gopinath, G. Veglia, Sensitivity enhancement in static solid-state NMR experiments via single- and multiple-quantum dipolar coherences, J. Am. Chem. Soc. 131 (2009) 5754-5756.
[28] T. Gopinath, R. Verardi, N. J. Traaseth, G. Veglia, Sensitivity enhancement of separated local field experiments: Application to membrane proteins, J. Phys. Chem. B 114 (2010) 5089-5095.
[29] S. V. Dvinskikh, H. Zimmermann, A. Maliniak, D. Sandström, Measurements of motionally averaged heteronuclear dipolar couplings in MAS NMR using R-type recoupling, J. Magn. Reson. 168 (2004) 194-201.
[30] D. J. States, R. A. Haberkorn, D. J. Ruben, A two-dimensional nuclear overhauser experiment with pure absorption phase in four quadrants, J. Magn. Reson. 48 (1982) 286-292.

[31] M. H. Levitt, Symmetry-based pulse sequences in magic-angle spinning solid-state NMR, in: D. M. Grant, R. K. Harris, Eds. Encyclopedia of Magnetic Resonance vol. 9, John Wiley & Sons, Ltd, Chichester, (2002) 165-196.
[32] X. Zhao, W. Hoffbauer, J. S. auf der Günne, M. H. Levitt, Heteronuclear polarization transfer by symmetry-based recoupling sequences in solid-state NMR, Solid State Nucl. Magn. Reson. 26 (2004) 57-64.
[33] M. Bak, J. T. Rasmussen, N. C. Nielsen, SIMPSON: A general simulation program for solid-state NMR spectroscopy, J. Magn. Reson. 147 (2000) 296-330.
[34] X. Zhao, J. L. Sudmeier, W. W. Bachovchin, M. H. Levitt, Measurement of NH bond lengths by fast magic-angle spinning solid-state NMR spectroscopy: A new method for the quantification of hydrogen bonds, J. Am. Chem. Soc. 123 (2001) 11097-11098.
[35] F. A. Perras, Z. Wang, P. Naik, I. I. Slowing, M. Pruski, Natural abundance ^{17}O DNP NMR provides precise O−H distances and insights into the Brønsted acidity of heterogeneous catalysts, Angew. Chem. Int. Ed. 56 (2017) 9165-9169.
[36] M. Edén, Enhanced symmetry-based dipolar recoupling in solid-state NMR, Chem. Phys. Lett. 378 (2003) 55-64.
[37] A. Gansmüller, J.-P. Simorre, S. Hediger, Windowed R-R-PDLF recoupling: A flexible and reliable tool to characterize molecular dynamics, J. Magn. Reson. 234 (2013) 154-164.
[38] X. Lu, H. Zhang, M. Lu, A. J. Vega, G. Hou, T. Polenova, Improving dipolar recoupling for site-specific structural and dynamics studies in biosolids NMR: windowed RN-symmetry sequences, Phys. Chem. Chem. Phys. 18 (2016) 4035-4044.
[39] M. G. Munowitz, R. G. Griffin, G. Bodenhausen, T. H. Huang, Two-dimensional rotational spin-echo nuclear magnetic resonance in solids: Correlation of chemical shift and dipolar interactions, J. Am. Chem. Soc. 103 (1981) 2529-2533.
[40] M. Hohwy, C. P. Jaroniec, B. Reif, C. M. Rienstra, R. G. Griffin, Local structure and relaxation in solid-state NMR: accurate measurement of amide N−H bond lengths and H−N−H bond angles, J. Am. Chem. Soc. 122 (2000) 3218-3219.
[41] G. Hou, X. Lu, A. J. Vega, T. Polenova, Accurate measurement of heteronuclear dipolar couplings by phase-alternating R-symmetry (PARS) sequences in magic angle spinning NMR spectroscopy, J. Chem. Phys. 141 (2014) 104202.
[42] E. Nimerovsky, C. P. Soutar, A modification of γ-encoded RN symmetry pulses for increasing the scaling factor and more accurate measurements of the strong heteronuclear dipolar couplings, J. Magn. Reson. 319 (2020) 106827.
[43] J. J. Kinnun, A. Leftin, M. F. Brown, Solid-State NMR Spectroscopy for the Physical Chemistry Laboratory, J. Chem. Ed. 90 (2013) 123-128.
[44] V. S. Bajaj, P. C. A. van der Wel, R. G. Griffin, Observation of a low-temperature, dynamically driven structural transition in a polypeptide by solid-state NMR spectroscopy. J. Am. Chem. Soc. 131 (2009) 118-128.